2010 IEEE International Conference on Robotics and Automation
Anchorage Convention District
May 3-8, 2010, Anchorage, Alaska, USA

External Sensorless Dynamic Object Manipulation by a Dual Soft-Fingered Robotic Hand with Torsional Fingertip Motion

Kenji Tahara, Keigo Maruta and Motoji Yamamoto

Abstract— **This paper proposes a novel object manipulation method by using a dual soft-fingered robotic hand system, in which each fingertip has a torsional joint. By using the torsional motion of the fingertips, a novel 3-dimensional dynamic object manipulation without use of any external sensing can be achieved even though the hand system has only two fingers. Firstly, our proposed system, which includes contact models between each fingertip and surfaces of an object, is modeled. A rolling contact between each fingertip and the object surfaces can be allowed because our proposed system has soft and deformable hemispheric fingertips. Moreover, a torsional contact model between each fingertip and the object surfaces is newly proposed. It is based on an assumption that the torsional motion induces an elastic strain potential. Secondly, a dynamic object manipulation control method is designed. The control signal is composed of four parts, the one is for grasping the object stably, the second one is for controlling a position of the object, the third one is for controlling an attitude of the object, and the last one is for the torsional fingertip motion. A numerical simulation based on our model is performed, and a manipulation experiment by using our developed setup is performed. The usefulness of our proposed method is demonstrated through these results.**

I. INTRODUCTION

A multi-fingered robotic hand system to realize a dexterous object manipulation has been researched from the early stage of robotics, and it has been still now one of the most expected devices not only in robotics, but also in its applicable fields. Up to now, many robotic hand systems have been developed aiming at the realization of a dexterous manipulation [1], [2]. These hands tend to be complicated system. It is because that they should have possessed a large number of D.O.F. as many as a whole body humanoid robot, since they had been designed based on the configuration of a human hand. Moreover, many control schemes for them have been designed on the basis of a manipulation planning method through some kind of optimizations [3] except for several works [4], [5]. Therefore, there are still now some difficulties to put them into practical use, because such computational cost tends to be increased with the increase of the complexity of their configuration. Of course, we know that mimicking the configuration of a human hand for designing a robotic hand is one of the effective methods to realize a dexterous and versatile robotic hand system. However, on the other hand, an anti-anthropomorphic robotic hand system, which possesses our unavailable hand configuration, has a potential to acquire wider work space, higher dexterity and versatility compared to a real human hand. [6], [7].

In this paper, a novel soft-fingered robotic hand system, which possesses one of our unavailable hand configurations, is proposed. The system is composed of a pair of 3 D.O.F. fingers, in which each finger possesses a torsional joint at a soft and hemispheric fingertip. By using the torsional fingertip motion, a novel 3-dimensional dexterous object manipulation can be realized with dynamic stability even though the system has only two fingers. Firstly, a dynamical model of the overall object-finger system, which considers contact models between each fingertip and the object surfaces, is constructed. In the construction of the soft contact models, we consider not only a rolling contact, but also a new torsional contact between each soft fingertip and the object surfaces. The new torsional contact model presented here is based on an assumption that the torsional motion between each soft fingertip and the object surfaces induces a nonlinear spring-like elastic strain potential which depends on the softness of the fingertip. Secondly, a control input to realize a 3-dimensional dynamic object manipulation without use of any external sensing is designed. Our proposed controller is composed of four parts, the first part is for stable object grasping based on the "Blind Grasping" manner proposed by Arimoto *et al.* [4], [5], the second part is for controlling a position of the grasped object, the third part is for controlling an attitude of the grasped object around the z axis of the inertial frame, and the last part is for controlling an attitude of the grasped object around the torsional axis of the fingertip. Thirdly, a numerical simulation using our dynamical model is conducted to show the effectiveness of our proposed contact model and controller. Finally, a manipulation experiment using our developed setup is performed, and the usefulness of our proposed manipulation method is demonstrated through both results of the simulation and the experiment.

II. DUAL SOFT-FINGERED ROBOTIC HAND WITH TORSIONAL JOINTS

A dual soft-fingered robotic hand system presented here is shown in Fig. 1. A realization of several 3-dimensional object manipulations can be expected by using the torsional fingertip motion as shown in Fig. 2. In this study, we assume

This work was partially supported by Japan Society for the Promotion of Science (JSPS), Grant-in-Aid for Scientific Research (B) (20360117), and "the Kyushu University Research Superstar Program (SSP)", based on the budget of Kyushu University allocated under President's initiative.

K. Tahara is with the Institute for Advanced Study, Kyushu University, 744 Moto'oka, Nishi-ku, Fukuoka 819-0395, Japan tahara@ieee.org

K. Maruta is with the Graduate School of Engineering, Kyushu University, 744 Moto'oka, Nishi-ku, Fukuoka 819-0395, Japan maruta@mint.mech.kyushu-u.ac.jp

M. Yamamoto is with the Faculty of Engineering, Kyushu University, 744 Moto'oka, Nishi-ku, Fukuoka 819-0395, Japan yama@mech.kyushu-u.ac.jp

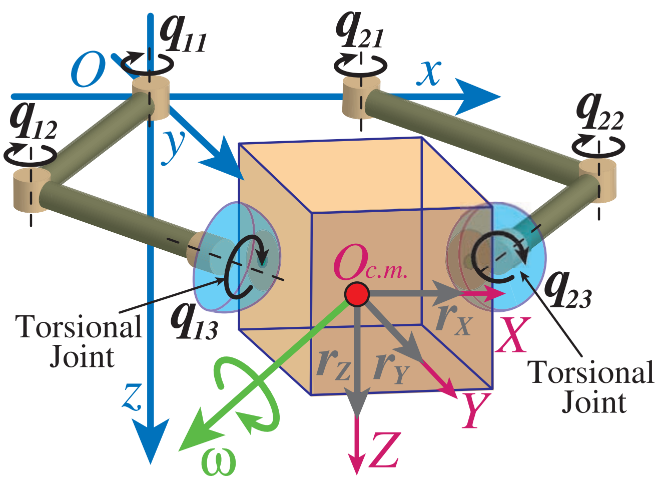

Fig. 1. Model of a dual soft-fingered robotic hand with torsional fingertip joints

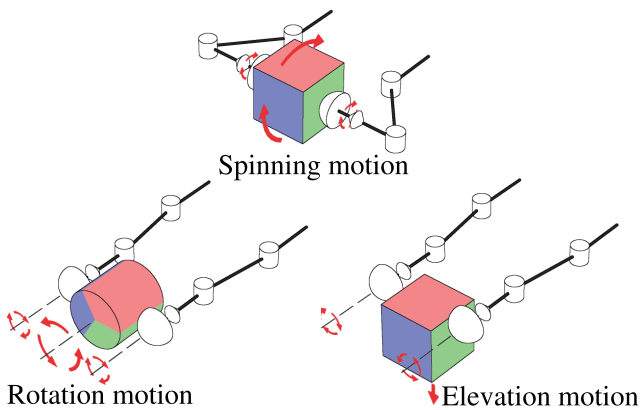

Fig. 2. Several expected 3-dimensional manipulations using the torsional fingertip motion

that a grasped object is a cuboid for the time being to model the overall system easier. Each finger has three joints which includes the torsional fingertip joint, and a joint angle vector for each finger is given as $\boldsymbol{q}_i = (q_{i1}, q_{i2}, q_{i3})^{\mathrm{T}} \in \mathbb{R}^3$ $(i = 1, 2)$, and q_{i3} denotes the torsional joint angle at each fingertip.

A. Rolling Contact Model toward the Tangential Direction of Contact Surfaces

Rolling constraints with area contact arise between each fingertip and the object surfaces, because each fingertip is made of some sort of soft material, and its shape is hemispheric. The condition of the rolling constraints can be expressed as one of the velocity constraints between each fingertip and the object surfaces [4], [5]. They are given in the following way:

$$\begin{bmatrix} (r_i - \Delta r_i)\boldsymbol{r_Y}^{\mathrm{T}}(\boldsymbol{\omega} - \boldsymbol{J}_{\omega i}\dot{\boldsymbol{q}}_i) = (-1)^i \dot{Z}_i \\ (r_i - \Delta r_i)\boldsymbol{r_Z}^{\mathrm{T}}(\boldsymbol{\omega} - \boldsymbol{J}_{\omega i}\dot{\boldsymbol{q}}_i) = -(-1)^i \dot{Y}_i \end{bmatrix}, \quad (i = 1, 2), \tag{1}$$

where r_i is a radius of each hemispheric fingertip, Δr_i is each fingertip's deformation displacement for normal direction on the contact surface, $\boldsymbol{\omega}$ is an angular velocity vector of the object expressed by the inertial frame, and $\boldsymbol{J}_{\omega i}$ is the Jacobian matrix for an attitude angular velocity of each fingertip with respect to each joint angular velocity vector $\dot{\boldsymbol{q}}_i$. Additionally, Y_i and Z_i are distances of which each length between the center of mass of the object $O_{c.m.} = (x, y, z)^{\mathrm{T}} \in \mathbb{R}^3$ and the center of each fingertip $\boldsymbol{x}_{0i} = (x_{0i}, y_{0i}, 0)^{\mathrm{T}} \in \mathbb{R}^2$ is projected to the Y and Z axes of the object local frame, respectively. They can be given in the following way:

$$\begin{bmatrix} Y_i = -\boldsymbol{r}_{\boldsymbol{Y}}^{\mathrm{T}}(\boldsymbol{x} - \boldsymbol{x}_{0i}) \\ Z_i = -\boldsymbol{r}_{\boldsymbol{Z}}^{\mathrm{T}}(\boldsymbol{x} - \boldsymbol{x}_{0i}) \end{bmatrix}, \quad (i = 1, 2), \tag{2}$$

where an attitude of the object in the inertial frame can be expressed by using the rotational matrix $\boldsymbol{R}$ such that

$$\boldsymbol{R} = (\boldsymbol{r_X},\ \boldsymbol{r_Y},\ \boldsymbol{r_Z}) \in SO(3). \tag{3}$$

In (3), $\boldsymbol{r_X}, \boldsymbol{r_Y}, \boldsymbol{r_Z} \in \mathbb{R}^3$ are mutually orthonormal vectors. The rolling constraint conditions expressed as (1) are non-holonomic, and they are of linear with respect to the related velocity vectors. Therefore, they can be expressed as Pfaffian constraints in the following way:

$$\begin{bmatrix} \boldsymbol{Y}_{qi}\dot{\boldsymbol{q}}_i + \boldsymbol{Y}_{xi}\dot{\boldsymbol{x}} + \boldsymbol{Y}_{\omega i}\boldsymbol{\omega} = 0 \\ \boldsymbol{Z}_{qi}\dot{\boldsymbol{q}}_i + \boldsymbol{Z}_{xi}\dot{\boldsymbol{x}} + \boldsymbol{Z}_{\omega i}\boldsymbol{\omega} = 0 \end{bmatrix}, \quad (i = 1, 2), \tag{4}$$

where

$$\begin{bmatrix} \boldsymbol{Y}_{qi} = -(r_i - \Delta r_i)\boldsymbol{r}_{\boldsymbol{Z}}^{\mathrm{T}}\boldsymbol{J}_{\omega i} + (-1)^i \boldsymbol{r}_{\boldsymbol{Y}}^{\mathrm{T}}\boldsymbol{J}_{0i} \\ \boldsymbol{Y}_{xi} = -(-1)^i \boldsymbol{r}_{\boldsymbol{Y}}^{\mathrm{T}} \\ \boldsymbol{Y}_{\omega i} = (r_i - \Delta r_i)\boldsymbol{r}_{\boldsymbol{Z}}^{\mathrm{T}} + (-1)^i(\boldsymbol{x} - \boldsymbol{x}_{0i})^{\mathrm{T}}[\boldsymbol{r_Y}\times] \end{bmatrix} \tag{5}$$

$$\begin{bmatrix} \boldsymbol{Z}_{qi} = -(r_i - \Delta r_i)\boldsymbol{r}_{\boldsymbol{Y}}^{\mathrm{T}}\boldsymbol{J}_{\omega i} - (-1)^i \boldsymbol{r}_{\boldsymbol{Z}}^{\mathrm{T}}\boldsymbol{J}_{0i} \\ \boldsymbol{Z}_{xi} = (-1)^i \boldsymbol{r}_{\boldsymbol{Z}}^{\mathrm{T}} \\ \boldsymbol{Z}_{\omega i} = (r_i - \Delta r_i)\boldsymbol{r}_{\boldsymbol{Z}}^{\mathrm{T}} - (-1)^i(\boldsymbol{x} - \boldsymbol{x}_{0i})^{\mathrm{T}}[\boldsymbol{r_Z}\times] \end{bmatrix}, \tag{6}$$

and the form of $[\cdot\times]$ signifies an operator that transforms a 3-dimensional vector to a skew-symmetric matrix. It means an operation of a vector product. Also, $\boldsymbol{J}_{0i}$ signifies the Jacobian matrix for the velocity of the center of each fingertip $\dot{\boldsymbol{x}}_{0i}$ with respect to each joint angular velocity $\dot{\boldsymbol{q}}_i$.

B. Soft Contact Model toward the Vertical Direction of Contact Surfaces

Each soft-fingertip's deformation displacement toward the normal direction on the contact surface can be expressed in the following way:

$$\Delta r_i = r_i + W_i + (-1)^i \boldsymbol{r_X}^{\mathrm{T}}(\boldsymbol{x} - \boldsymbol{x}_{0i}), \ (i = 1, 2), \tag{7}$$

where W_i is the distance of which a length between the center of mass of the object $O_{c.m.}$ and the center of each contact area $\boldsymbol{x}_{0i}$ is projected to the X axis of the object local frame. It means $W_1 + W_2$ is the width of the object. In this paper, we introduce the lumped-parameterized contact model for the deformation of the fingertip at the center of each contact area that has been proposed by Arimoto *et al.* [8]. A reaction force f_i at the center of the contact area according to the lumped-parameterized contact model is given as follows:

$$f_i = k_{fi}\Delta r_i^2 + b_{fi}\Delta\dot{r}_i, \quad (i = 1, 2), \tag{8}$$

where k_{fi} and b_{fi} are an elastic and viscosity coefficient respectively, and these depend on a material and a contact area.

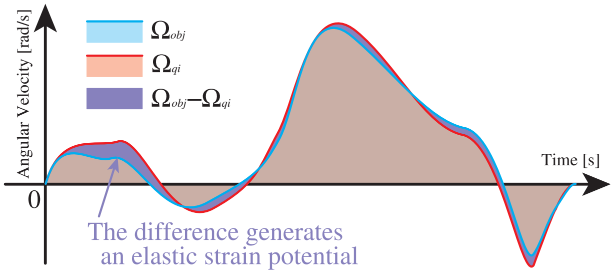

Fig. 3. Schematic graph of the generation of the torsional elastic strain potential

C. Soft Contact Model toward the Torsional Direction of Fingertips

In this paper, a new soft contact model toward the torsional direction on the contact surface is modeled. Assume that a torsional motion between each soft fingertip and the object surfaces induces an elastic strain. A nonlinear spring-like potential caused by the elastic strain is expressed as an approximated model in the following way:

$$K_{\omega i} = \frac{k_{\omega i}}{2} \left\| \boldsymbol{\Omega}_{obj} - \boldsymbol{\Omega}_{qi} \right\|^2, \quad (i = 1, 2), \tag{9}$$

$$\left[\boldsymbol{\Omega}_{obj} = \int_0^t \boldsymbol{\omega} \mathrm{d}t \in \mathbb{R}^3, \quad \boldsymbol{\Omega}_{qi} = \int_0^t \boldsymbol{J}_{\omega i} \dot{\boldsymbol{q}}_i \mathrm{d}t \in \mathbb{R}^3 \right.$$

where $k_{\omega i}$ is a torsional elastic coefficient which depends on a material and contact area. Note that the time integration of the object angular velocity vector $\boldsymbol{\omega}$ and each fingertip angular velocity vector $\boldsymbol{J}_{\omega i}\dot{\boldsymbol{q}}_i$ on the right-hand side of (9) indicate not each attitude angle, but each path length of the center of the contact area from time $t \in [0, t)$. Namely, this contact model indicates that an elastic strain potential is generated by the difference between a path length of the center of the contact area on the fingertip and that on the object surface, as shown schematically in Fig. 3. In addition to the elastic strain potential, we model a torsional damping effect to dissipate the elastic strain potential energy. It is given as follows:

$$T_{\omega i} = \frac{b_{\omega i}}{2} \left\| \boldsymbol{\omega} - \boldsymbol{J}_{\omega i} \dot{\boldsymbol{q}}_i \right\|^2, \quad (i = 1, 2), \tag{10}$$

where $b_{\omega i}$ is a viscosity coefficient which depends on a material and a contact area. Eventually, the physical interaction between the fingertip and the object surfaces with respect to the torsional fingertip motion is defined by the elastic strain potential expressed by (9) and the energy dissipation function expressed by (10).

D. DYNAMICS

The overall dynamics, which consider all the contact models presented in the previous section, can be represented in the following way:

For the robotic fingers:

$$\begin{aligned} \boldsymbol{H}_i \ddot{\boldsymbol{q}}_i + \left\{ \frac{1}{2} \dot{\boldsymbol{H}}_i + \boldsymbol{S}_i \right\} \dot{\boldsymbol{q}}_i + \boldsymbol{Y}_{qi}^{\mathrm{T}} \lambda_{Yi} + \boldsymbol{Z}_{qi}^{\mathrm{T}} \lambda_{Zi} \\ -(-1)^i \boldsymbol{J}_{0i}^{\mathrm{T}} \boldsymbol{r}_{\boldsymbol{X}} f_i + k_{\omega i} \boldsymbol{\Delta J}_{\omega i}^{\mathrm{T}} \left(\boldsymbol{\Omega}_{qi} - \boldsymbol{\Omega}_{obj} \right) \\ + b_{\omega i} \boldsymbol{J}_{\omega i}^{\mathrm{T}} \left(\boldsymbol{J}_{\omega i} \dot{\boldsymbol{q}}_i - \boldsymbol{\omega} \right) = \boldsymbol{u}_i, \quad (i = 1, 2) \end{aligned} \tag{11}$$

For the object:

$$\boldsymbol{M}\ddot{\boldsymbol{x}} + \sum_{i=1}^{2} \left\{ \boldsymbol{Y}_{xi}^{\mathrm{T}} \lambda_{Yi} + \boldsymbol{Z}_{xi}^{\mathrm{T}} \lambda_{Zi} + (-1)^i \boldsymbol{r}_{\boldsymbol{X}}^{\mathrm{T}} f_i \right\} + \boldsymbol{g} = \boldsymbol{0} \tag{12}$$

$$\begin{aligned} \boldsymbol{I}\dot{\boldsymbol{\omega}} + [\boldsymbol{\omega} \times] \boldsymbol{I} \boldsymbol{\omega} + \sum_{i=1}^{2} \Big\{ \boldsymbol{Y}_{\omega i}^{\mathrm{T}} \lambda_{Yi} + \boldsymbol{Z}_{\omega i}^{\mathrm{T}} \lambda_{Zi} \\ + (-1)^i [\boldsymbol{r}_{\boldsymbol{X}} \times] (\boldsymbol{x} - \boldsymbol{x}_{0i}) f_i + k_{\omega i} \left(\boldsymbol{\Omega}_{obj} - \boldsymbol{\Omega}_{qi} \right) \\ + b_{\omega i} \left(\boldsymbol{\omega} - \boldsymbol{J}_{\omega i} \dot{\boldsymbol{q}}_i \right) \Big\} = \boldsymbol{0}, \end{aligned} \tag{13}$$

where $\boldsymbol{H}_i$ and $\boldsymbol{M}$ stand for inertia matrices for the finger and the object respectively, $\boldsymbol{S}_i$ is a skew-symmetric matrix, $\boldsymbol{\Delta J}_{\omega i}^{\mathrm{T}} = (\boldsymbol{J}_{\omega i}(t) - \boldsymbol{J}_{\omega i}(0))^{\mathrm{T}}$, $\boldsymbol{I} = \boldsymbol{R}^{\mathrm{T}} \bar{\boldsymbol{I}} \boldsymbol{R}$ and $\bar{\boldsymbol{I}}$ is an inertia tensor of the object represented by the principal axes of inertia. The gravity term affect to the object is $\boldsymbol{g} = (0, 0, g)^{\mathrm{T}}$. On the other hand, the robotic fingers system does not possess joints affected by the gravity. Also, λ_{Yi} and λ_{Zi} denote rolling constraint forces toward Y and Z axis of the local object frame, respectively.

III. CONTROL LAW

A control signal to realize a stable object grasping, an object position control, an object attitude control around the z axis of the inertial frame, and an object attitude control around the torsional axis of the fingertip is designed here. In this study, the control input is constructed by four components expressed below [4], [5].

- $\boldsymbol{u}_s$: To grasp the object stably
- $\boldsymbol{u}_{\tilde{x}}$: To control the virtual object position
- $\boldsymbol{u}_{\tilde{\theta}}$: To control the virtual object attitude around the z axis of the inertial frame
- $\boldsymbol{u}_{\alpha}$: To control the torsional fingertip joint angle

Note that the objective of our proposed controller is to manipulate an object not accurately, but roughly. Accordingly, the total control input presented here can be constructed only by using available information such as each joint angle and angular velocity. It means that any external sensing information is unnecessary for our proposed controller. Therefore in the construction of $\boldsymbol{u}_{\tilde{x}}$ and $\boldsymbol{u}_{\tilde{\theta}}$, we introduce a virtual object position $\tilde{\boldsymbol{x}}$ and a virtual object attitude around the z axis of the inertial frame $\tilde{\theta}$, instead of the real information regarding the object. The virtual position $\tilde{\boldsymbol{x}}$ is defined as the middle position between each center of the fingertip. The virtual attitude $\tilde{\theta}$ is defined as the tilt angle of a line segment that connects each center of the fingertip with respect to the inertial frame. They are given in the following way:

$$\tilde{\boldsymbol{x}} = \frac{\boldsymbol{x}_{01} + \boldsymbol{x}_{02}}{2}, \qquad \tilde{\theta} = \tan^{-1} \left(\frac{y_{02} - y_{01}}{x_{02} - x_{01}} \right) \tag{14}$$

Each concrete control input is constructed easily in the following way:

$$\left[\begin{aligned} \boldsymbol{u}_{si} &= (-1)^i \frac{f_d}{\|\boldsymbol{\Delta x}_0\|} \boldsymbol{J}_{0i}^{\mathrm{T}} \boldsymbol{\Delta x}_0 \\ \boldsymbol{u}_{\tilde{x}i} &= -\boldsymbol{J}_{0i}^{\mathrm{T}} \left(\boldsymbol{K}_{px} \boldsymbol{\Delta} \tilde{\boldsymbol{x}} + \boldsymbol{K}_{vx} \dot{\tilde{\boldsymbol{x}}} \right) \\ \boldsymbol{u}_{\tilde{\theta}i} &= -\frac{K_{p\theta}}{\|\boldsymbol{\Delta x}_0\|} \boldsymbol{J}_{0i}^{\mathrm{T}} \boldsymbol{J}_{\theta i}^{\mathrm{T}} \Delta \tilde{\theta} \\ \boldsymbol{u}_{\alpha i} &= -\boldsymbol{K}_{p\alpha} \boldsymbol{\Delta \alpha}_i \end{aligned} \right. , (i = 1, 2) \tag{15}$$

where f_d stands for a desired grasping force, $\boldsymbol{K}_{px} = \mathrm{diag}(k_{px}, k_{py}, 0)^{\mathrm{T}} > \boldsymbol{0} \in \mathbb{R}^3$, $\boldsymbol{K}_{vx} = \mathrm{diag}(k_{vx}, k_{vy}, 0)^{\mathrm{T}} > \boldsymbol{0} \in \mathbb{R}^3$, $K_{p\theta} > \boldsymbol{0} \in \mathbb{R}^1$, $\boldsymbol{K}_{p\alpha} = \mathrm{diag}(0, 0, k_{p\alpha})^{\mathrm{T}} > \boldsymbol{0} \in \mathbb{R}^3$ signify each gain. Additionally, $\boldsymbol{\Delta x}_0$, $\boldsymbol{\Delta \tilde{x}}$, $\Delta\tilde{\theta}$, $\boldsymbol{\Delta\alpha}_i$, $\boldsymbol{\alpha}_i$, and $\boldsymbol{J}_{\theta i}$ denote below.

$$\left[\begin{array}{l} \boldsymbol{\Delta x}_0 = \boldsymbol{x}_{01} - \boldsymbol{x}_{02}, \ \boldsymbol{\Delta\tilde{x}} = \boldsymbol{\tilde{x}} - \boldsymbol{x}_d \\ \boldsymbol{J}_{\theta i} = \dfrac{(-1)^i}{\|\boldsymbol{\Delta x}_0\|}\begin{pmatrix} y_{02} - y_{01} \\ x_{01} - x_{02} \end{pmatrix}^{\mathrm{T}}, \ \Delta\tilde{\theta} = \tilde{\theta} - \theta_d \\ \boldsymbol{\alpha}_i = (0, \ 0, \ q_{i3})^{\mathrm{T}}, \ \boldsymbol{\Delta\alpha}_i = \boldsymbol{\alpha}_i - \boldsymbol{\alpha}_{di} \end{array}\right. \quad (i = 1, 2). \tag{16}$$

In this paper, the desired torsional joint angle for each finger is given as $\boldsymbol{\alpha}_{d1} = -\boldsymbol{\alpha}_{d2}$. It means the sign of desired angle for each fingertip is opposite, but its absolute value is the same. Eventually, the control input can be given by the summation of each element shown in (15) with a joint damping term in the following way:

$$\boldsymbol{u}_i = -\boldsymbol{C}_i\dot{\boldsymbol{q}}_i + \boldsymbol{u}_{si} + \boldsymbol{u}_{\tilde{x}i} + \boldsymbol{u}_{\tilde{\theta}i} + \boldsymbol{u}_{\alpha i}, \ (i = 1, 2), \tag{17}$$

where $\boldsymbol{C}_i = \mathrm{diag}(c_{i1}, c_{i2}, c_{i3}) > \boldsymbol{0}$ denotes a joint damping matrix.

IV. NUMERICAL SIMULATION

Each parameter used in a numerical simulation is stated in Table I. In the simulation, a desired virtual object position $\boldsymbol{\tilde{x}}$, a desired virtual object attitude $\tilde{\theta}$, and a desired torsional fingertip joint angle q_{i3d} are given as a point, and which are changed according to time t. Transient responses of $\boldsymbol{\tilde{x}}$, $\tilde{\theta}$, and q_{i3} in the simulation are shown in Fig. 4. We see from this figure that $\boldsymbol{\tilde{x}}$ converges to the desired value, and $\tilde{\theta}$ and q_{i3} mostly converge to the desired angle with small steady state errors. These small errors are induced by the elastic strain potential as shown in (9). Additionally, the object grasping force f_i, the rolling constraint forces λ_{Yi} and λ_{Zi}, and the elastic strain potential caused by the torsional motion of each fingertip $K_{\omega i}$ are shown in Fig. 5. We see from this figure that f_d is realized, and λ_{Yi} and λ_{Zi} converge to zero, respectively. On the other hand, $K_{\omega i}$ is apt to be generated when each finger's attitude becomes asymmetric with respect to the position of the object. It is because that as shown in Fig. 6, the locus of each center of contact area on the object surface becomes a circle, and its radius depends on the contact approach angle between the fingertip and the object surface. The difference of each radius of torsional fingertip motion on the object surface as shown in Fig. 7 makes the difference of the rolling distance per revolution of the fingertip. Therefore, the object spinning motion around each torsional joint of the fingertip makes a discrepancy when the radius of each fingertip torsional motion is different. This discrepancy induces elastic strain potentials at both the fingertips. Also, we can conclude from the simulation result that these elastic strain potentials do not diverge to infinity as long as each fingertip torsional joint is not rotated to the same direction continuously. Therefore, we conclude that our proposed model is enough to express adequately the torsional motion of the fingertip around the neighborhood of the initial condition.

TABLE I

PARAMETERS USED IN THE SIMULATION

Robotic fingers system	
1st link length l_{i1}	0.070 [m]
2nd link length l_{i2}	0.030 [m]
3rd link length l_{i3}	0.024 [m]
1st link mass m_{i1}	0.31 [kg]
2nd link mass m_{i2}	0.31 [kg]
3rd link mass m_{i3}	0.14 [kg]
r_i	0.015 [m]
k_{fi}	2.0×10^5
$k_{\omega i}$	1.0×10^2
b_{fi}	$1000 \times (2r_i\Delta r_i - \Delta r_i^2)\pi$
$b_{\omega i}$	$30 \times (2r_i\Delta r_i - \Delta r_i^2)\pi$
Object	
Mass	0.0021 [kg]
Size	0.048×0.048×0.048 [m]
Desired grasping force and each gain	
f_d	0.5 [N]
$\boldsymbol{K}_{px}$	diag(200, 200, 0)
$\boldsymbol{K}_{vx}$	diag(200, 200, 0)
$K_{p\theta}$	10
$\boldsymbol{K}_{p\alpha}$	diag(0, 0, 0.1)
$\boldsymbol{C}_i$	diag(0.1, 0.1, 2.0)×10^{-2}
Initial condition	
$\boldsymbol{q}_1$	$(2.13, -1.64, 0.0)^{\mathrm{T}}$ [rad]
$\boldsymbol{q}_2$	$(1.01, 1.64, 0.0)^{\mathrm{T}}$ [rad]
$\boldsymbol{x}$	(0.050, 0.085, 0.0) [m]

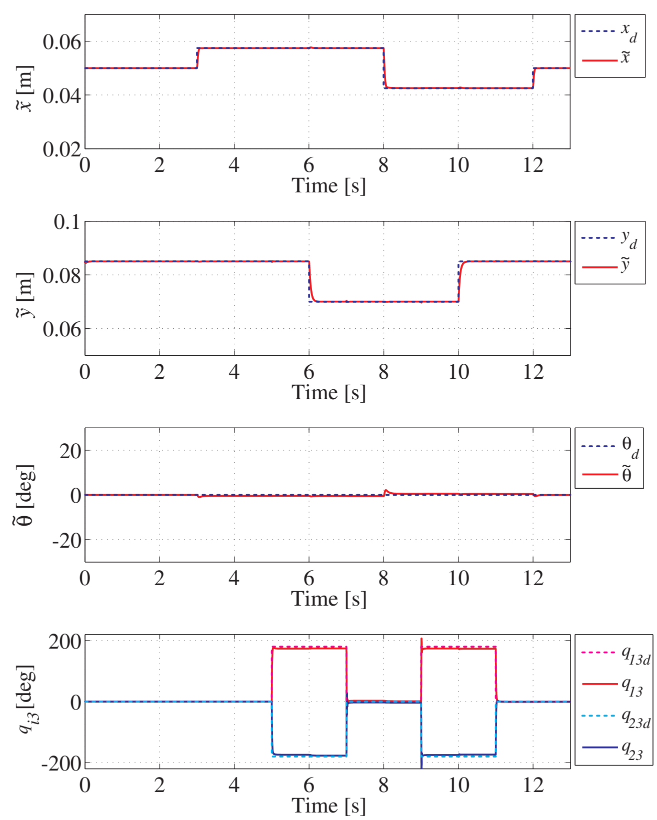

Fig. 4. Simulation result of the virtual object position $\boldsymbol{\tilde{x}}$, the virtual object angle $\tilde{\theta}$, and the torsional angle q_{i3} for each fingertip

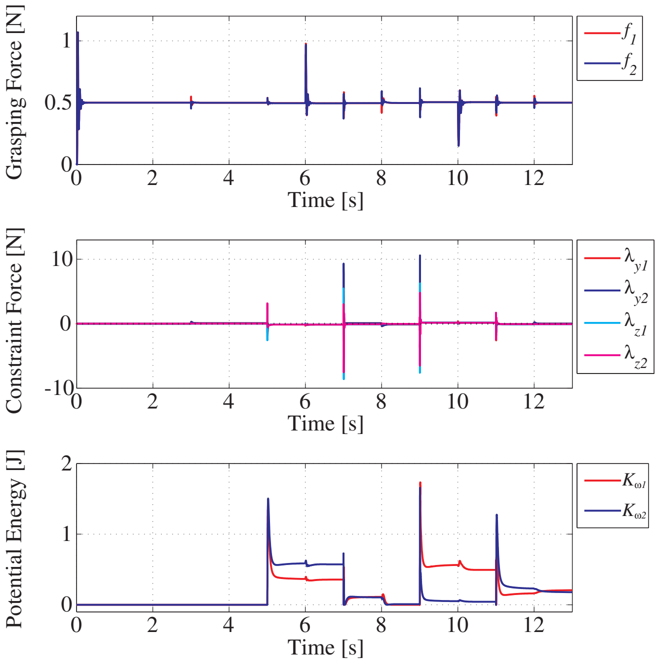

Fig. 5. Simulation results of the grasping force f_i, the rolling constraint forces λ_{Y_i}, λ_{Z_i}, and the torsional elastic strain potential $K_{\omega i}$ for each fingertip

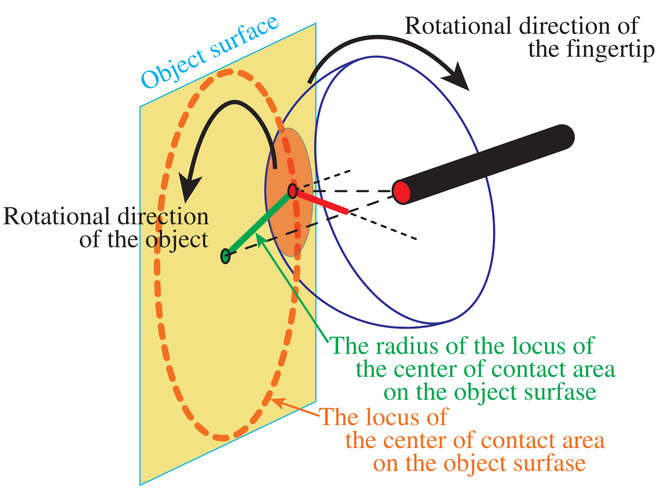

Fig. 6. Locus of each center of contact area becomes a circle on the object surface

V. EXPERIMENT

In this section, we perform a manipulation experiment by using our developed robotic hand system. A schematic view of our developed experimental setup is shown in Fig. 8, and a picture of that of a real one is also shown in Fig. 9. Our developed system has 3 D.O.F. for each finger, which has the torsional joint at the soft and hemispheric fingertip. Joints of each finger are driven by geared motors installed at the base of the system, and the generated torques by the geared motors are transmitted to each joint by a timing belt. The hemispheric fingertips are made of soft polyurethane. All gains and the desired values of the virtual object position $\boldsymbol{x}_d$, the virtual object attitude θ_d, and the torsional joint

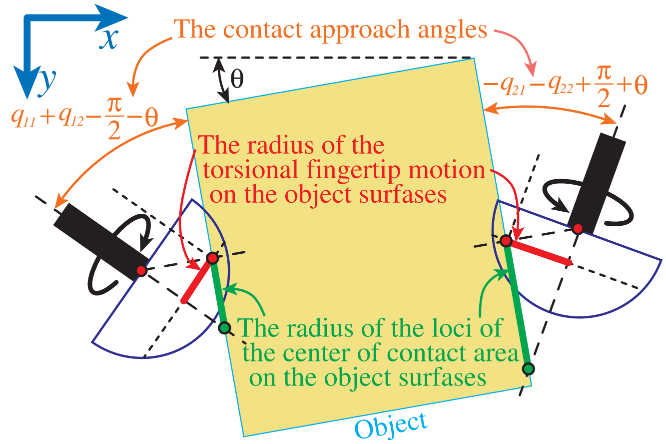

Fig. 7. Difference of the rolling distance per revolution of the fingertip between each fingertip due to the defference of each contact approach angle

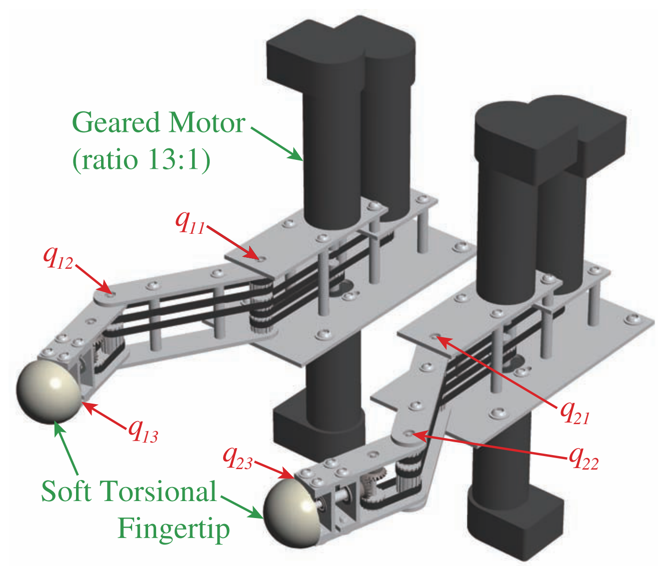

Fig. 8. Schematic view of a dual soft-fingered robotic hand with torsional fingertip joints

angle of each fingertip q_{i3d} are set to the same values used in the numerical simulation. A photographic strip during the manipulation experiment is shown in Fig. 10. Transient responses of the virtual object position $\tilde{\boldsymbol{x}}$, the virtual object attitude $\tilde{\theta}$, and the torsional joint angle of each fingertip q_{i3} for the object manipulation experiment are shown in Fig.11. We see from these figures that the external sensorless 3-dimensional object manipulation with dynamic stability can be realized by using our proposed controller and the system. Additionally, the transient response of each variable is quite similar to the numerical simulation results. Therefore, we can conclude that our proposed contact model can express the torsional motion of the fingertip, adequately.

VI. CONCLUSION

In this paper, we proposed a novel robotic fingers system, which has two fingers and each fingertip possess the torsional joint. Through the results of both the numerical simulation

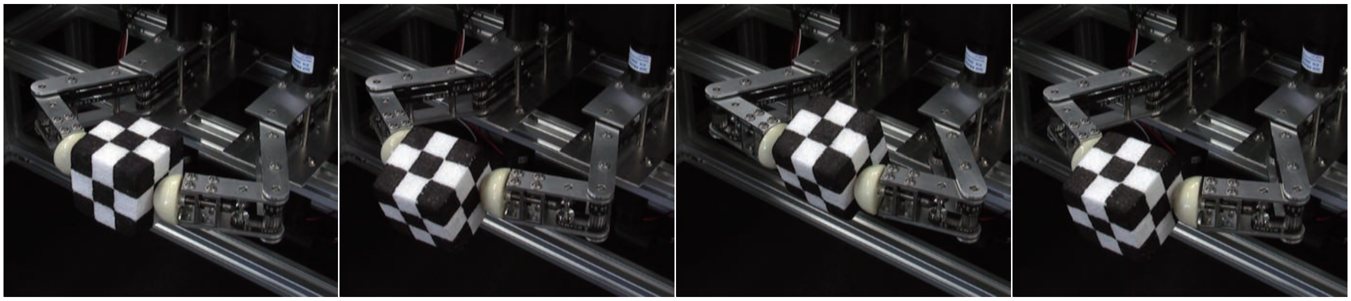

∼2 [s] ∼6 [s] ∼10 [s] ∼13 [s]

Fig. 10. Photographic strip during a manipulation experiment

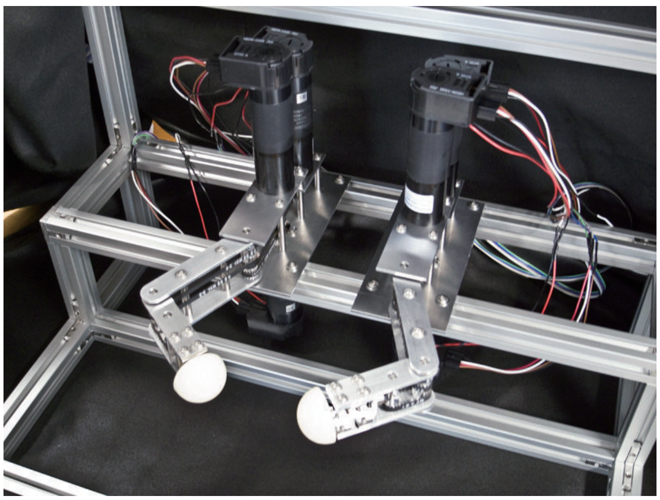

Fig. 9. Experimental setup of a dual soft-fingered robotic hand with torsional fingertip joints

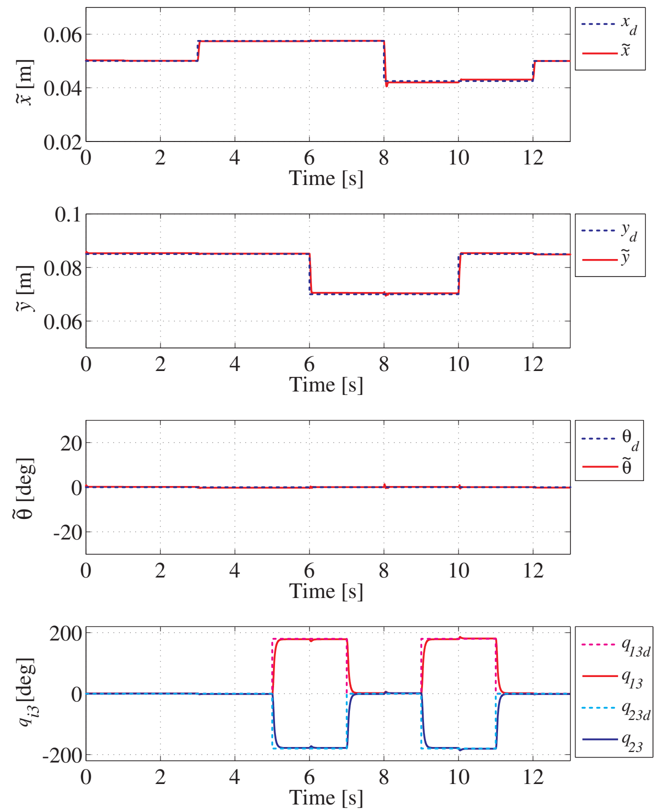

Fig. 11. Experimental result of the virtual object position $\tilde{\boldsymbol{x}}$, the virtual object angle $\tilde{\theta}$, and the torsional angle q_{i3} for each fingertip

and the experiment, we conclude that by using the torsional fingertip motion, the 3-dimensional dynamic object manipulation can be realized without use of any external sensing, even the system possesses only two fingers. Additionally, our proposed contact model was quite effective to express sufficiently the interactive movement between both fingertips and the object in the dynamical sense, by comparing the results between the numerical simulation and the experiment. In our future works, the convergence of the overall system will be illustrated. Also, the relation between the attitude of an object and the torsional motion of the fingertip should be analyzed from both analytical and experimental viewpoints in more detail.

ACKNOWLEDGMENT

This work was partially supported by Japan Society for the Promotion of Science (JSPS), Grant-in-Aid for Scientific Research (B) (20360117), and "the Kyushu University Research Superstar Program (SSP)", based on the budget of Kyushu University allocated under President's initiative.

REFERENCES

[1] C. Borst, M. Fischer, S. Haidacher, H. Liu and G. Hirzinger, "DLR Hand II: Experiments and experiences with an anthropomorphic hand," *Proc. IEEE Int. Conf. Robot. Automat.*, pp. 702–707, 2003.

[2] K. Kaneko, K. Harada, and F. Kanehiro, "Development of multi-fingered hand for life-size humanoid robots," *Proc. IEEE Int. Conf. Robot. Automat.*, pp. 913–920, 2007.

[3] K.B. Shimoga, "Robot grasp synthesis algorithms: A survey," *Int. J. Robot. Res.*, vol. 15, no. 3, pp. 230–266, 1996.

[4] S. Arimoto, M. Yoshida and J.-H. Bae, "Stable blind graspin of a 3-D object under non-holonomic constraints," *Proc. IEEE Int. Conf. Robot. Automat.*, pp. 2124–2130, 2006

[5] S. Arimoto, "A differential-geometric approach for 2-D and 3-D object grasping and manipulation," *Annual Review in Control*, Vol. 31, pp. 189–209, 2007.

[6] K. Nagata, "Manipulation by a parallel-jaw gripper having a turntable at each fingertip," *Proc. IEEE Int. Conf. Robot. Automat.*, pp. 1663-1670, 1994.

[7] A. Bicchi, A. Marigo and D. Prattichizzo, "Dexterity through rolling: Manipulation of unknown objects," *Proc. IEEE Int. Conf. Robot. Automat.*, pp. 1583–1588 , 1999.

[8] S. Arimoto, P.T.A. Nguyen, H.-Y. Han and Z. Doulgeri, "Dynamics and control of a set of dual fingers with soft tips," *Robotica*, vol. 18, no. 1, pp. 71–80, 2000.